Cement and Concrete Research 174 (2023) 107334

Contents lists available at ScienceDirect

Cement and Concrete Research

journal homepage: www.elsevier.com/locate/cemconres

Internal alkali transport in recycling concrete and its impact on alkali-silica reaction

Andreas Leemann [a,b,*], Leandro Sanchez [c]

[a] Empa, Swiss Federal Laboratories for Materials Science and Technology, Überlandstrasse 129, 8600 Dübendorf, Switzerland
[b] School of Geography and Environmental Sciences, Ulster University, Coleraine BT52 1SA, Northern Ireland, UK
[c] Department of Civil Engineering, University of Ottawa, 161 Louis-Pasteur Private, Ottawa, ON K1N 6N5, Canada

ARTICLE INFO

Keywords:
Recycled concrete aggregates
Alkali-silica reaction
Microstructure
Pore solution

ABSTRACT

Recycling concrete (RC) produced with recycled aggregates (RA) obtained from demolished concrete structures bears the risk of an alkali-silica reaction (ASR). In this study, the interplay between aggregate reactivity and alkalis contributed by the cement and the RA is investigated. Three sets of concrete mixtures are produced using RA and natural aggregates, both reactive and non-reactive ones. Caesium either present in the RA or in the mixing water of the RC is used to trace the transport of alkalis and their incorporation in ASR products. The result shows that alkali released by RA can intensify ASR. On the other hand, ASR in RA with a low alkali content but reactive aggregate particles can be triggered by the alkali provided by the new cement paste of the RC. The highest risk of ASR in RC is caused by RA from a source concrete already affected by ASR.

1. Introduction

Producing recycled aggregates (RA) from demolished concrete is a mandatory step towards circular economy in the construction industry [1–3]. The use of RA in recycling concrete (RC) is an established technique in numerous countries [4]. Typically, RA and natural aggregates are combined in the production of RC [5–7]. However, amongst the challenges of using RA in concrete is the presence of mineral phases prone to develop alkali-silica reaction (ASR), a deleterious physico-chemical reaction affecting concrete infrastructure worldwide. It has been shown in past studies that reactive aggregates present in RA can lead to induced expansion and cracking of recycling concrete [8–17]. Typically, the alkali concentration in both RA and RC is similar in such studies; therefore, it is difficult to assess the role of the alkalis already present in the RA and the alkalis provided by the cement of the newly produced RC on the development of expansion and cracking. This study focuses then on the impact of different alkali levels in the RA and cement paste of the newly produced RC on the development of ASR. The three following scenarios are investigated:

Scenario A: The RA (composed of the original natural aggregates and residual cement paste) contains a high alkali concentration and a non-reactive original natural aggregate. Consequently, the demolished concrete exhibits no signs of ASR. When RC is produced with this RA combined with a new reactive natural aggregate and a new cement paste with an inferior (i.e., let's say a moderate) alkali level, the alkalis provided by the RA may lead to a reaction with the new reactive natural aggregate (Fig. 1, images A).

Scenario B: The RA contains a very inferior (i.e., low) alkali level and reactive original natural aggregates. As a result, the demolished concrete does not display signs of ASR-induced deterioration. If the RC is produced with a cement paste of high alkali level, these new alkalis may trigger ASR in the RA containing reactive NA (Fig. 1, images B).

Scenario C: The RA contains a moderate to high alkali level and reactive RA. Accordingly, the demolished concrete presents some damage due to ASR. Here, the question that arises is on the impact of the alkali level of the new cement paste on the potential for further ASR-induced expansion and cracking (Fig. 1, images C). If the RC is produced with a low level of alkalis in the new cement paste, then the alkalis present in the RA may not be sufficient to sustain further reaction. However, it can be expected that if the alkali level in the cement paste of the RC is high, further expansion will occur.

Three different RA were fabricated for the production of seven different RC covering the three scenarios abovementioned (Fig. 1). As caesium (Cs) was incorporated to the mixture, the formation of new ASR products could be tracked, which helps the understanding of the alkalis transport in the system; Cs was added to the concrete in two distinct

* Corresponding author at: Empa, Laboratory for Concrete & Asphalt, Überlandstrasse 129, CH-8600 Dübendorf, Switzerland.
E-mail address: andreas.leemann@empa.ch (A. Leemann).

https://doi.org/10.1016/j.cemconres.2023.107334
Received 23 June 2023; Received in revised form 21 August 2023; Accepted 13 September 2023

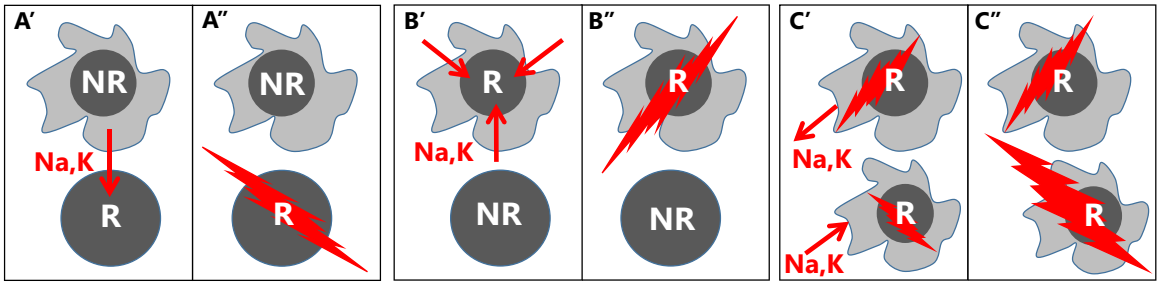

Fig. 1. Alkali transport from RA to reactive natural aggregates (scenario A), from the new cement paste to reactive RA (scenario B) and the residual expansion potential of RA from an already previously ASR-damaged concrete possibly affected by the alkali level of the new cement paste (scenario C).

Table 1
Composition of PC-1, PC-2 and the limestone powder (LP).

	SiO_2	Al_2O_3	Fe_2O_3	Cr_2O_3	MnO	TiO_2	P_2O_5	CaO	MgO	K_2O	Na_2O	SO_3	LOI	TC
	[mass%]													
PC-1	20.9	4.98	3.18	0.01	0.06	0.26	0.17	65.5	1.86	0.88	0.16	3.02	1.16	0.50
PC-2	19.97	4.41	3.53	–	0.06	0.19	0.15	62.1	2.67	0.90	0.40	4.00	1.90	–
LP	<0.11	<0.11	<0.04	<0.003	–	<0.02	0.05	55.4	0.52	<0.03	<0.03	0.10	43.7	13.3

Table 2
Density and Blaine values of PC-1, PC-2 and LP.

	Density [g/cm^3]	Blaine [cm^2/g]
PC-1	3.16	4180
PC-2	3.17	3930
Limestone powder	2.72	4970

Table 3
Mix design of the concrete used for the production of RA.

		RA-NR	RA-R-1	RA-R-2
PC-1	[kg/m^3]	330	215	–
PC-2	[kg/m^3]	–	–	420
Limestone powder	[kg/m^3]	–	115	–
NaOH addition	[kg/m^3]	–	–	1.84
$CsNO_3$ addition	[kg/m^3]	6.0	–	–
Water	[kg/m^3]	182	182	189
Aggregate NR-1 0–4 mm	[kg/m^3]	642	–	–
Aggregate NR-1 4–22 mm	[kg/m^3]	1192	–	–
Aggregate R-1 0–4 mm	[kg/m^3]	–	642	–
Aggregate R-1 4–22 mm	[kg/m^3]	–	1192	–
Aggregate NR-2 0–4.5 mm	[kg/m^3]	–	–	823
Aggregate R-2 4.5–19.5 mm	[kg/m^3]	–	–	934
Na_2Oeq	*[kg/m^3]*	*3.39*	*1.59*	*5.25*
cement paste	*[l/m^3]*	*289*	*293*	*321*
w/p	*[–]*	*0.55*	*0.55*	*0.45*
Compressive strength at 56 days	*[MPa]*	*40.9*	*31.0*	–

ways: a) in the concrete used for RA production and, b) to the mixing water of the RC. RC specimens were manufactured according to the concrete prism test and ASR-induced expansion was monitored over time. The composition of ASR products was analyzed with scanning electron microscopy (SEM) and energy-dispersive X-ray spectroscopy (EDS). Additionally, two mortars were produced, one of them containing Cs-bearing RA. Their pore solution was extracted at different ages to assess the contribution of the alkalis present in the RA to the total pore solution.

2. Materials and methods

2.1. Materials

Two different Portland cements (PC-1 and PC-2) and limestone powder (LP) were used for the production of RA and concrete. PC-2 was only used for the production of recycled aggregate RA-R-2. Composition, density and Blaine values of PC-1, PC-2 and LP are shown in Tables 1 and 2.

Concrete was produced with four different natural aggregates. The first natural aggregate (NR-1) consists of a well-rounded alluvial sand and gravel mainly composed of limestone and sandstone with siliceous limestone, quartzite, and gneiss as minor components; its susceptibility to ASR is low. The second natural aggregate (NR-2) is a non-reactive crushed sand consisting of quartz, feldspar, calcite, and dolomite. The third natural aggregate (R-1) is a crushed sandstone containing quartz, feldspar, carbonates, and layered silicates. The presence of minor amount of detritic chert and amorphous SiO_2 leads to a very high ASR susceptibility. In the Swiss concrete prism test [18] that is similar to RILEM AAR-4.1 [19] a concrete produced with 375 kg/m^3 Portland cement, a water-to-cement-ratio of 0.45 and aggregate R-1 reaches an expansion of 0.47 ‰ after 20 weeks, which is over twice as much of the allowed limit. The fourth and last natural aggregate (R-2) is a crushed stone from Canada (Springhill) and bears a similar composition to the aggregate R-1 but with a smaller amount of quartz; its ASR susceptibility is also very high [16,17,20]. Natural aggregates NR-1 and R-1 were used for the production of the RA and the RC mixtures (Tables 3 and 4), while natural aggregates NA-2 and R-2 were only used for the production of RA.

Three different RA were produced, derived from concrete mixtures RA-NR, RA-R-1 and RA-R-2 (Table 3). Concrete mixture RA-NR, incorporating the non-reactive natural aggregate NR, was boosted with $CsNO_3$ to reach a high alkali level (3.39 % of Na_2O_{eq}, scenario A). Concrete mixture RA-R-1, bearing the highly reactive aggregate R-1, was proportioned with a low alkali level (1.59 % of Na_2O_{eq}, scenario B). The concrete mixture RA-R-2, incorporating the highly reactive aggregate R-2, was mix-proportioned with a high alkali content (i.e., 5.25 of Na_2O_{eq}, scenario C, as per ASTM C-1293 [21] or CSA.A23.2-14A [22]) following the approach as specified in [16,17,20].

2.2. Concrete mixture proportioning and RC samples preparation

Twenty cubes with a side length of 150 mm and three 70 × 70 × 280 mm^3 prisms were produced with aggregates NR and R-1. Upon demoulding, the cubes were stored at 20 °C and >95 % relative humidity (RH) over 56 days and then crushed to produce RA. The compressive strength of the cubes measured at 56 days was 40.9 and

Table 4
Mix design of the RC. NR = non-reactive, R = reactive, RA = recycled concrete aggregates.

Concrete	–	A1	A2	A3[a]	B1	B2	C1	C2
PC-1	[kg/m^3]	370	370	370	370	370	240	370
Limestone powder	[kg/m^3]	–	–	–	–	–	130	–
$CsNO_3$ addition	[kg/m^3]	–	–	–	6.71	6.71		6.71
Water	[kg/m^3]	178	178	178	178	178	178	178
Aggregate NR-1 0–4 mm	[kg/m^3]	–	–	318	318	637	631	636
Aggregate NR-1 4–22 mm	[kg/m^3]	–	–	592	592	592	–	–
Aggregate R-1 0–4 mm	[kg/m^3]	318	637	318	–	–	–	–
Aggregate R-1 4–22 mm	[kg/m^3]	592	592	592	–	–	–	–
Aggregate RA-NR 0–4 mm	[kg/m^3]	281		–	–	–	–	–
Aggregate RA-NR 4–22 mm	[kg/m^3]	521	521	–	–	–	–	–
Aggregate RA-R-1 0–4 mm	[kg/m^3]	–	–	–	281	–	–	–
Aggregate RA-R-1 4–22 mm	[kg/m^3]	–	–	–	521	521	–	–
Aggregate RA-R-2 5–19 mm	[kg/m^3]	–	–	–	–	–	1018	1028
Na_2Oeq without RA	[kg/m^3]	2.7	2.7	2.7	3.8	3.8	1.8	3.8
Na_2Oeq with RA	[kg/m^3]	3.4	3.2	2.7	4.3	4.1	4.1	6.1
cement paste without RA	[l/m^3]	298	298	298	300	300	306	300
cement paste in RA	[l/m^3]	100	74	–	100	74	136	137
w/p	[–]	0.48	0.48	0.48	0.48	0.48	0.48	0.48
Compressive strength at 28 days	[MPa]	43.1	47.6	50.9	39.4	45.0	35.7	30.1

[a] A3 is not a RC but rather a conventional concrete.

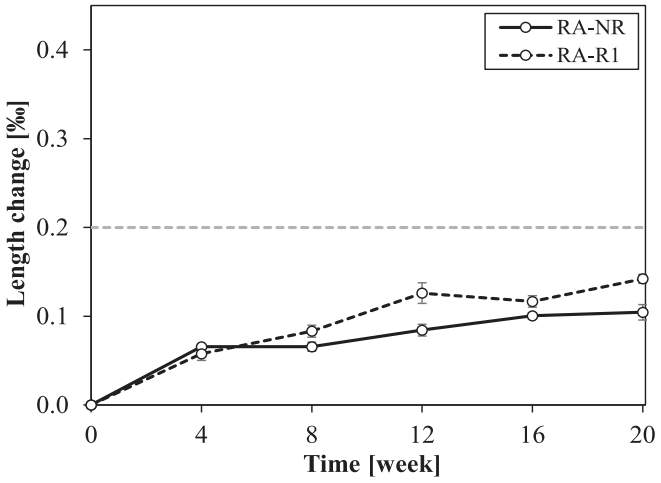

Fig. 2. Length change as a function of time of the source concrete for the production of recycled aggregate RA-NR and RA-R-1.

30.1 MPa, respectively for NR and R-1 mixtures (Table 3). Otherwise, the prisms were used to perform the concrete prism test as per [18] to appraise their expansive potential. The length change of the prisms at the end of the test (i.e., 20 weeks) was well below the limit value of proposed by [18] (i.e., 0.2 ‰ at 20 weeks; further information on the CPT method are presented in Section 2.3.2) (Fig. 2). Therefore, it is assumed that no to very little reaction took place in the cubes stored at 20 °C when compared to the already low results obtained at 60 °C in the concrete prism test. The crushed material was sieved into four distinct gradations: 0–4, 4–8, 8–16, and 16–32 mm. Likewise, 100 mm by 200 mm cylinders were produced incorporating the highly reactive R-2 aggregate and stored at 38 °C and 100 % RH. The cylinders were monitored over time and crushed when the concrete reached an expansion of 3.0 ‰ after 23 weeks. The aggregate gradations reached via sieving for this aggregate were 4.75–9, 9–12.5 and 12.5–19 mm. As no material was discarded, the volume of cement paste in the RA corresponds to the one of the concrete before crushing (Table 3).

The mix design of the RC mixtures is given in Table 4. Three prisms ($70 \times 70 \times 280$ mm^3) for the CPT and one cube with a side length of 150 mm for compressive strength testing were produced from each of the three mixtures. The compressive strength of the cube was measured after 28 days according to [23] (Table 4). The representative standard deviation for the compressive strength of concrete cubes derived from three

Table 5
Mix design of the mortars used for pore solution extraction. cp = cement paste.

Mortar	PC-1 [kg/m^3]	Water [kg/m^3]	w/c [–]	Aggregate NR-1 0–4 mm [kg/m^3]	Aggregate RA-NR 0–4 mm [kg/m^3]	Na_2O_{eq} without RA [kg/m^3]	Na_2O_{eq} with RA [kg/m^3]	Na_2O_{eq} per cp [kg/m^3]
M	666	320	0.48	1230	–	4.9	4.9	9.2
MC	666	320	0.48	575	575	4.9	5.7	9.5

Table 6
Composition of the pore solution of mortar M and mortar MC containing 50 mass% of aggregate RA-NR.

	Time [days]	Na	K	Cs	Ca	Cl	NO_3	SO_4	Si	Na + K + Cs	pH	(Na + K)/Cs
		[mmol/l]										
Mortar M	1	72.2	281.2	n.a.	2.58	4.26	0.02	8.91	0.03	353.3	13.30	–
	7	93.1	308.3	n.a.	2.28	0.94	0.02	3.47	0.03	401.5	13.35	–
	28	111.6	374.1	n.a.	2.73	1.04	0.03	6.64	0.03	485.8	13.42	–
	56	134.1	400.0	n.a.	3.03	0.75	0.03	9.90	0.04	534.1	13.43	–
Mortar MC	1	72.8	274.1	20.5	2.60	4.17	0.49	11.9	0.04	367.4	13.38	16.9
	7	93.3	312.6	30.1	1.59	1.14	1.49	4.83	0.02	436.0	13.43	13.5
	28	99.8	352.2	20.1	2.54	1.21	3.58	7.31	0.08	472.1	13.42	22.5
	56	116.8	367.1	22.6	1.91	1.10	3.39	10.9	0.04	506.5	13.45	21.4

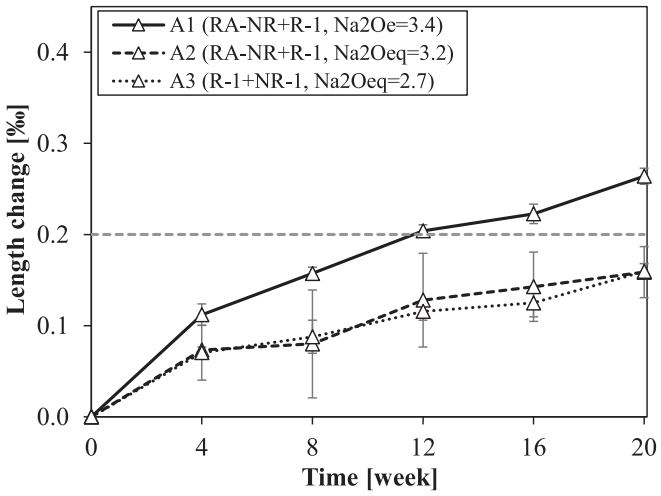

Fig. 3. Length change as a function of time for concrete A1, A2 and A3. The dotted grey line indicates the limit value. The Na_2Oeq of the concrete is given in kg/m^3.

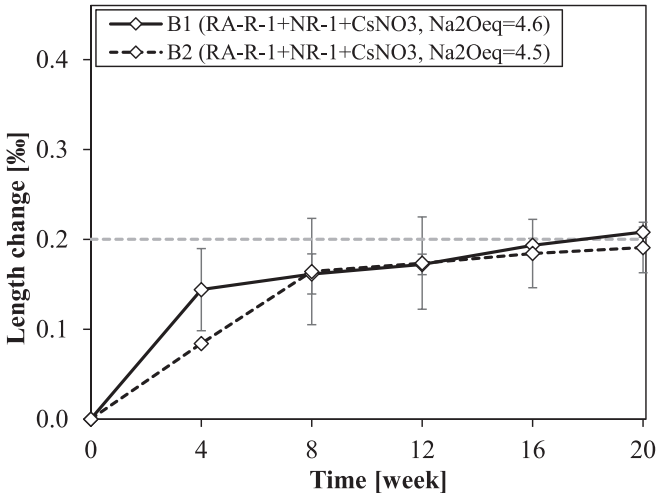

Fig. 4. Length change as a function of time for concrete B1 and B2. The dotted grey line indicates the limit value. The Na_2Oeq of the concrete is given in kg/m^3.

cubes of 40 different concrete mixtures is ±0.8 MPa. Additionally, mortars were produced using the mix-proportions displayed in Table 5. Right after mixing, the mortars were poured into plastic bottles with a volume of about 0.7 l. They were closed with air-tight screw-tops, sealed in zip-lock bags and stored in an oven at 60 °C until pore solution extraction.

The Na_2O_{eq} of the concrete and mortars, not accounting for the alkalis in the RA is defined as low (<2.0 kg/m^3), moderate (2.0–3.0 kg/m^3) and high (>3.0 kg/m^3) as illustrated in Table 4. This definition was chosen according to [24].

2.3. Methods

2.3.1. Pore solution extraction

The pore solution of mortar samples was collected through the steel die method, using pressure values up to 520 MPa after 1, 7, 28 and 56 days. The solutions were immediately filtered using 0.45 µm nylon filters. After filtration, an aliquot was diluted with HNO_3 (6.5 %) to prevent the precipitation of solids. pH measurements were conducted on the remaining solution with a pH electrode previously calibrated using

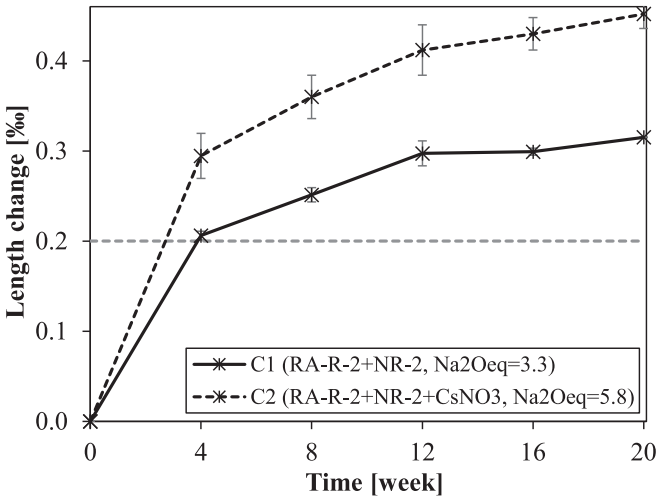

Fig. 5. Length change as a function of time for concrete C1 and C2. The dotted grey line indicates the limit value. The Na_2Oeq of the concrete is given in kg/m^3.

KOH solutions of known concentrations. The concentrations of Na, K, Cs, Ca, N, Al, S, and Si were measured via ion chromatography (IC). Pore solution analysis was performed at 1, 7, 28 and 56 days after the mortars' production.

2.3.2. Concrete prism test (CPT)

The CPT according to the Swiss standard [18] was performed on the concrete prisms; the protocol requires storage of the prims (70 × 70 × 280 mm) at 60 °C and 100 % relative humidity (RH) for 20 weeks with measurements every 4 weeks. The limit value of expansion as specified in the Swiss guideline 2042 is 0.20 ‰. The repeatability of the method is 0.027 ‰ [25].

2.3.3. Microstructure analysis

The samples for the microstructural analysis were cut, oven dried at 50 °C for three days, epoxy impregnated, polished and carbon coated. Their analysis was performed with a scanning electron microscope (SEM) FEI Quanta 650 using a pressure between 3.0 and 4.0 × 10^{-6} Torr. Elemental analysis was conducted by energy dispersive X-ray spectroscopy (EDS) with a Thermo Noran Ultra Dry 60mm^2 detector and Pathfinder X-Ray Microanalysis Software. An acceleration voltage of 12 kV and a spot size of 4.5 were used for imaging and EDS point analysis. Acceleration voltage and spot size were increased for the elemental maps to 20 kV and 5, respectively. All concentrations are given in at.%. Analysis of the concrete mixtures A1, A2, B1 and C2 was performed after 20 weeks. Concrete mixtures C1 and C2 were additionally analyzed after 6 weeks. To increase reliability of the data gathered, 200–250 data points from ASR secondary products encountered in at least 6 aggregates within each concrete sample were analyzed by EDS. All presented images were acquired in the back-scattering mode.

3. Results

3.1. Pore solution

Cs and NO_3 added in the production of RA-NR are present in the extracted pore solution of mortar MC (Table 6). The concentration of NO_3 is considerably lower than the one of Cs, indicating NO_3 absorption by cement hydrates. Moreover, it is interesting to note that the sum of Na and K is about 18 times higher, on average, than the concentration of Cs. Both the pH and alkali concentration in the pore solution of mortar M and MC are slightly increasing from 1 to 56 days. The concentrations are comparable in both mortars.

Table 7
Composition of the ASR products formed in aggregates at the age of 6 weeks (only concrete C1 and C2 as indicated) and 20 weeks.

Concrete	O	Na	Mg	Al	Si	K	Ca	Fe	Cs	Ca/Si	(Na + K + Cs)/Si	Na/K
	[at.%]									[−]		
A1 amorphous	64.8	1.9	0.1	0.4	21.9	4.3	6.0	0.1	0.5	0.28	0.30	0.44
	±3.2	±0.7	±0.1	±0.8	±1.9	±0.9	±1.2	±0.1	±0.1	±0.03	±0.04	±0.09
A1 crystalline	66.3	0.4	0.1	0.3	22.5	5.1	4.9	0.1	0.4	0.22	0.26	0.14
	±3.3	±0.4	±0.1	±1.4	±1.8	±1.2	±0.8	±0.1	±0.3	±0.03	±0.06	±0.85
A2 amorphous	67.3	1.6	0.2	0.2	20.9	4.5	4.8	0.2	0.4	0.23	0.31	0.34
	±3.1	±1.1	±0.5	±0.2	±1.8	±0.8	±0.6	±0.3	±0.1	±0.02	±0.09	±0.23
B1	65.4	1.7	0.1	0.4	22.2	2.6	6.3	0.1	1.3	0.28	0.25	0.68
	±2.8	±0.5	±0.1	±0.4	±1.9	±0.6	±1.1	±0.1	±0.3	±0.05	±0.05	±0.22
C1, 6w	66.9	2.1	0.3	0.3	20.8	4.7	4.6	0.3	0.0	±0.22	0.34	0.51
	±3.9	±0.5	±0.1	±0.2	±2.6	±1.9	±1.1	±0.1	0.0	±0.04	±0.11	±0.18
C2, 6w	66.2	2.0	0.2	0.4	21.1	3.9	4.6	0.3	1.3	0.21	0.34	0.52
	±4.0	±0.6	±0.2	±0.8	±3.3	±1.0	±2.2	±0.2	±0.3	±0.09	±0.06	±0.17
C2	65.8	2.1	0.2	0.2	22.9	3.9	3.1	0.3	1.4	0.14	0.33	0.56
	±3.6	±0.7	±0.2	±0.3	±2.4	±1.0	±1.9	±0.2	±0.3	±0.08	±0.08	±0.16

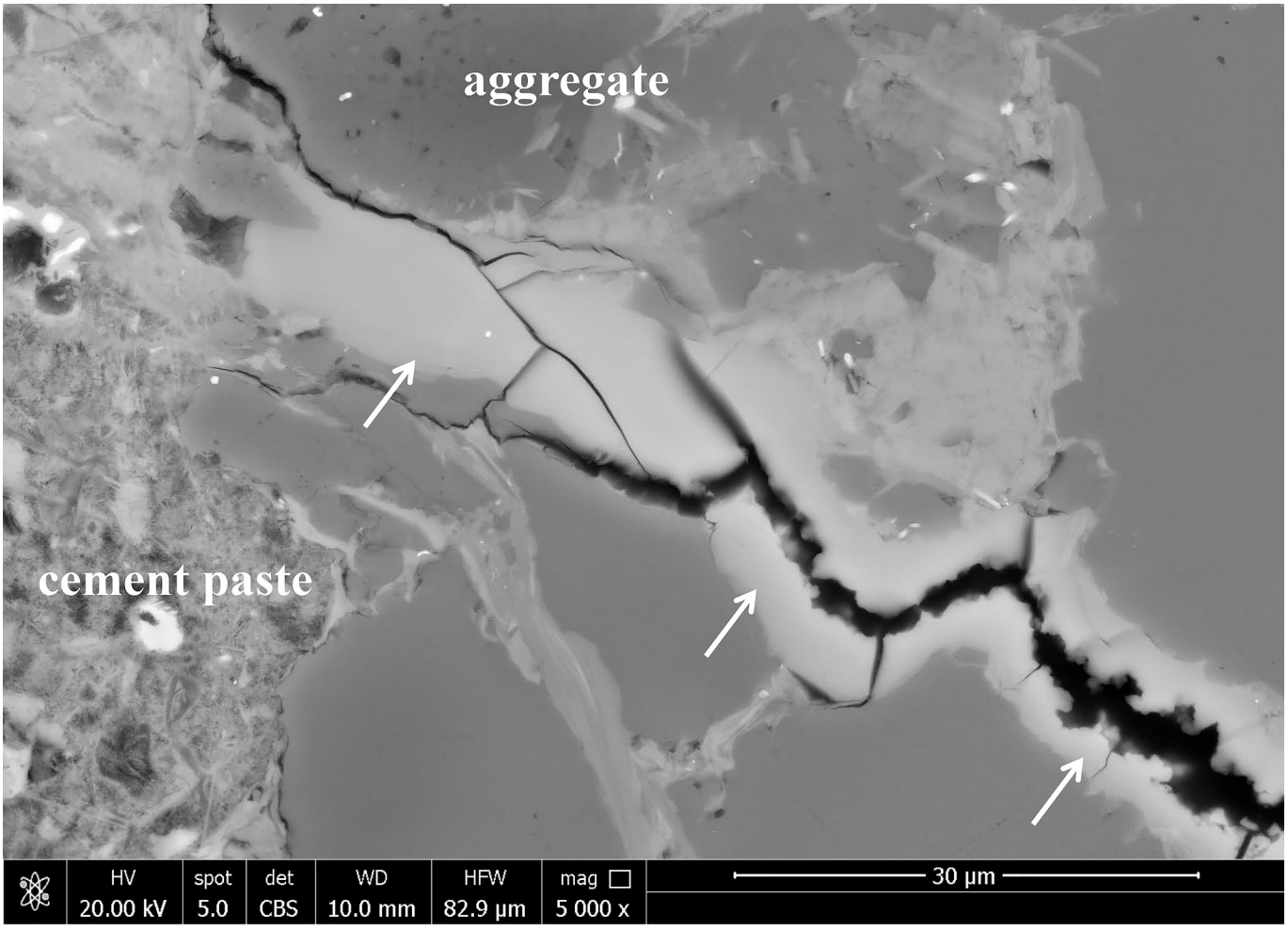

Fig. 6. Cs-containing amorphous ASR product (white arrows) in a crack formed in aggregate R-1. Concrete A1 at 20 weeks. Cs originally contained in recycled aggregate RA-NR.

3.2. Concrete prism test (CPT)

3.2.1. Scenario A

In scenario A, the concrete mixture A3 (i.e., conventional concrete) containing 50 mass% of the natural reactive aggregate R-1 and 50 mass % of the natural non-reactive aggregate NR-1, shows an expansion just below the limit value (Fig. 3). Whenever the natural non-reactive aggregate NR-1 is replaced by the recycled aggregate RA-NR, there is an increase in the Na_2O_{eq} of the RC which leads to a more pronounced reaction of natural aggregate R-1 resulting in a higher expansion of concrete A1. Otherwise, if only 32.5 mass% of natural aggregate NR-1 is replaced instead of 50 mass% by omitting the fine aggregates portion of the mixture, the expansion is not increased (concrete A2).

3.2.2. Scenario B

When recycled aggregate RA-R-1 bearing a low alkali level is used to

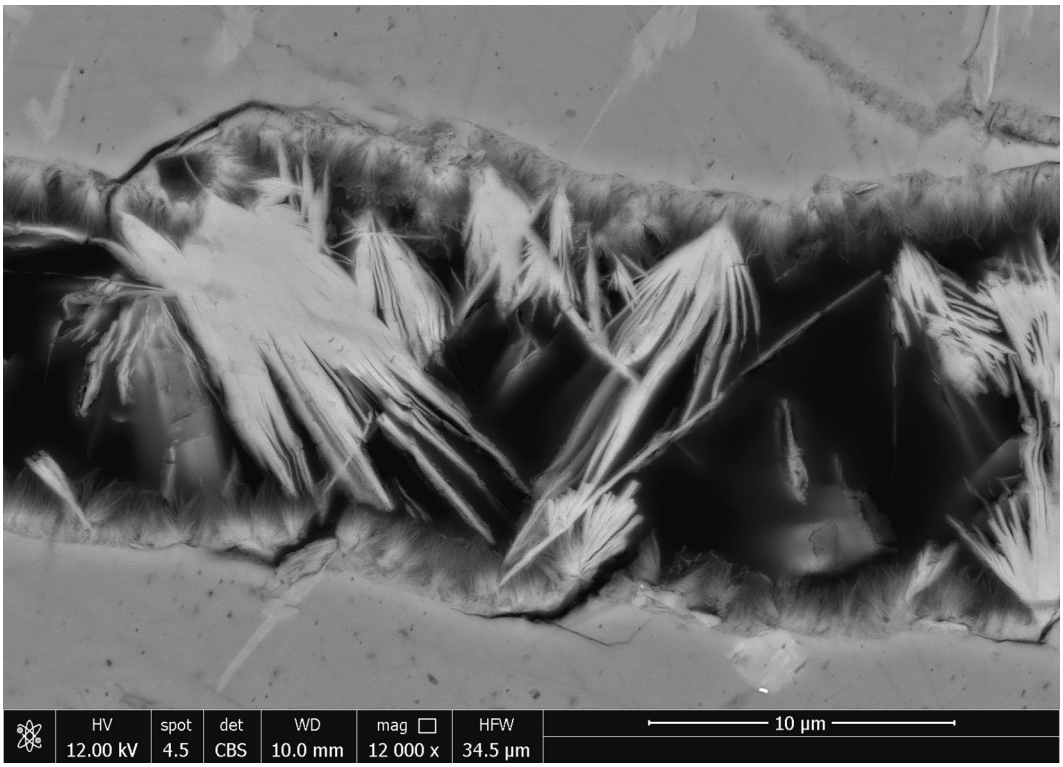

Fig. 7. Cs-containing crystalline ASR product in a crack formed in aggregate R-1. Concrete A1 at 20 weeks. Cs originally contained in recycled aggregate RA-NR.

produce a recycling concrete with a high alkali content, an expansion close to the threshold value takes place (i.e., B1 mixture) (Fig. 4). However, whenever the sand fraction 0–4 mm of recycled aggregate is not used in concrete mixture (i.e., B2 mixture), the expansion is lower after 4 weeks but increases to about the same level than B1 after 20 weeks.

3.2.3. Scenario C

Aggregate RA-R-2 with a high alkali level and already reacted aggregates is used in two RC mixtures, with low high alkali contents in the new cement paste following scenario C. Despite the low alkali level in the new cement paste, concrete prims proportioned with mixture C1 still swell well above the threshold value (Fig. 5). An even more pronounced expansion is present by the prisms from concrete mixture C2 due to the higher alkali content of the new cement paste.

3.3. ASR products

3.3.1. Scenario A

There are no signs of ASR in the Cs-bearing recycled aggregate RA-NR in concrete mixtures A1 and A2. However, cracks filed by ASR products starting in the natural reactive aggregate R-1 and running into the cement paste were observed. EDS analysis confirms the presence of Cs in these products (Table 7, Fig. 6). Typically, the back-scattering contrast of quartz and ASR products is identical, but in concrete mixtures A1 and A2, they display a higher contrast resulting in a lighter grey when compared to quartz due to the high atomic number of Cs (Fig. 6). Furthermore, amorphous and crystalline ASR products can be clearly distinguished in concrete A1. The crystalline product (Fig. 7) contains significantly less Na (Na/K-ratio of 0.14) than the amorphous product (Na/K-ratio of 0.44) confirming previous findings [26]. Nevertheless, both crystalline and amorphous products found in concrete mixture A1 contain Cs. The increased back-scattering contrast due to the incorporation of Cs allows to easily identify ASR products in yet uncracked aggregates as described in [27].

Most of the ASR products formed in the aggregate particles of concrete A2, which in turn swells less than concrete mixture A1, are amorphous or cryptocrystalline (platelets with a size < 1 µm) with very little crystalline products.

3.3.2. Scenario B

Amorphous and cryptocrystalline ASR products form in the aggregates RA-R-1 of concrete B1 (Figs. 8 and 9). There are some extrusions of ASR products accumulating in pores of the interface between the recycled aggregate RA-R-1 and the new cement paste (Fig. 10). The ASR products composition formed within the aggregates is very similar to the one measured in concrete mixtures A1 and A2; yet two differences were observed. First, the Cs content is about three times higher (Table 7). This corresponds to the higher Cs content of concrete B1 as a result of the $CsNO_3$ addition to the mixing water. The Cs content of concrete B1 is

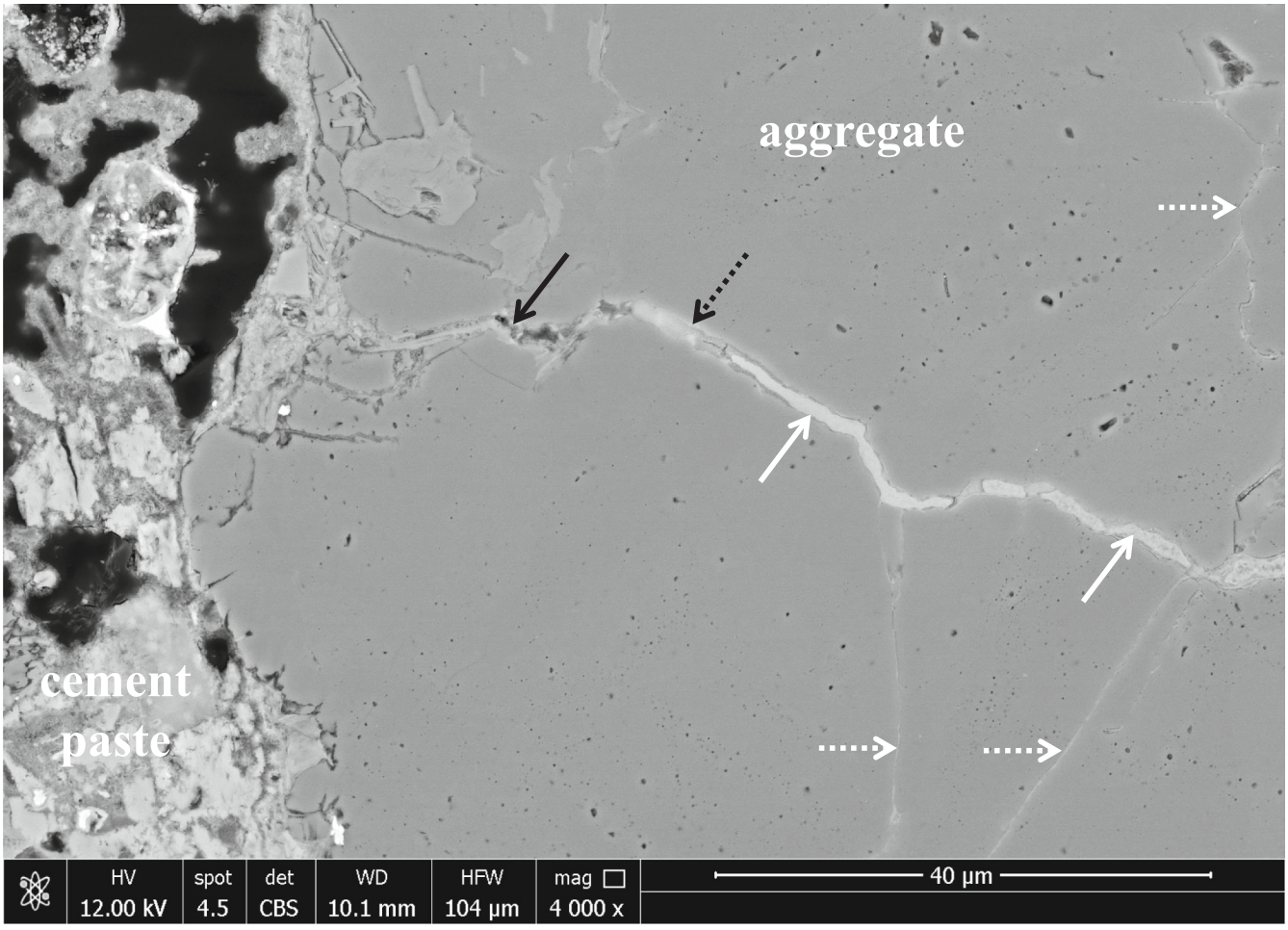

Fig. 8. Aggregate RA-R-1 with original cement paste and natural aggregate R-1 in concrete B1 at 20 weeks. The crack close to the ITZ with the cement paste is partly filled with low Ca/Si-ratio C-S-H (black arrow), followed by a transition zone with a mix of C-S-H and ASR product (dotted black arrow), before the crack is filled with Cs-containing ASR products (white arrows) as described in [27]. Some microcracks and gaps between adjacent quartz grains with a width in the range of 150 nm are filled with Cs-containing ASR products (dotted white arrows). Cs added to the mixing water.

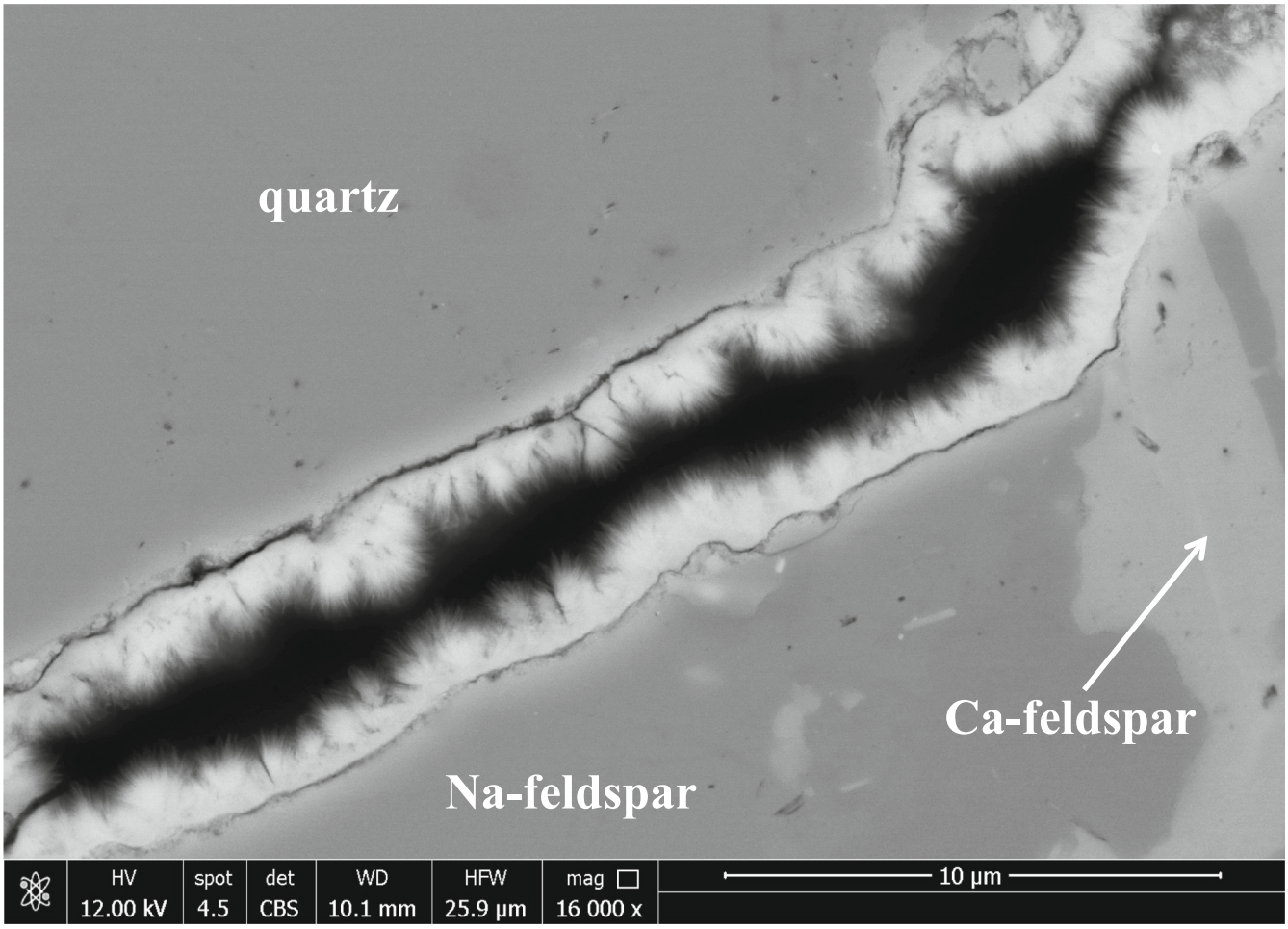

Fig. 9. Cs-containing amorphous and cryptocrystalline ASR products formed in a crack of recycled aggregate RA-R-1. Concrete B1 at 20 weeks. Cs added to the mixing water.

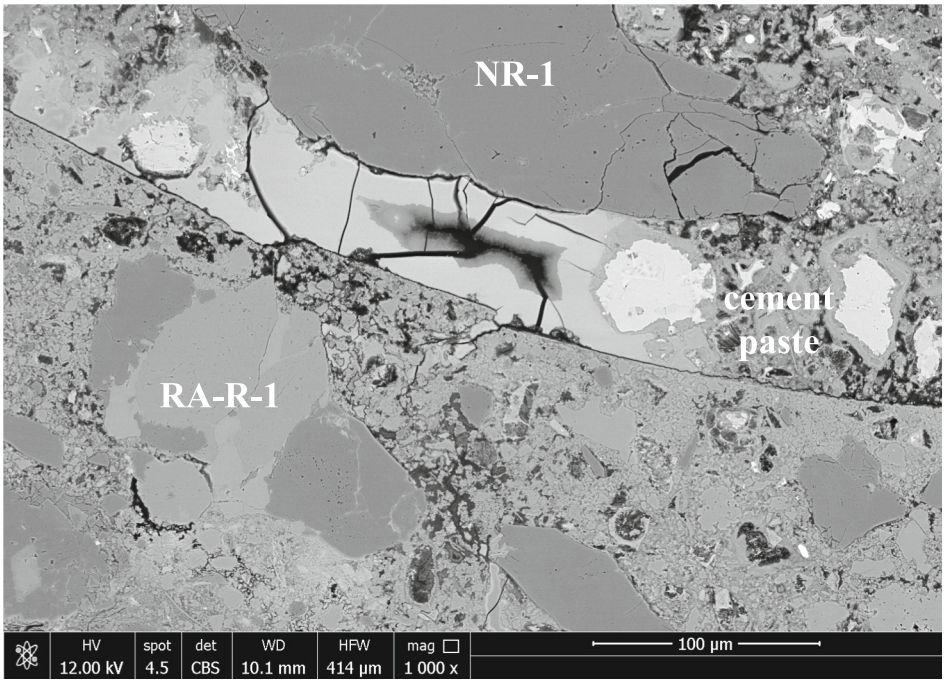

Fig. 10. Void at the interface between recycled aggregate RA-R-1 and the new cement paste filled with Cs-containing amorphous ASR products extruded from aggregate RA-R-1. Concrete B1 at 20 weeks. Cs added to the mixing water.

equal to 34 mol/m^3, while the ones of concrete mixtures A1 and A2 are 10 and 8 mol/m^3, respectively. Secondly, the K content in the ASR products from B1 mixture is lower than concrete mixtures A1 and A2, leading to a higher Na/K-ratio (Fig. 11).

3.3.3. Scenario C

Amorphous ASR products are present in the aggregates of concrete mixtures C1 and C2 after an age of 6 weeks. It can be assumed that these products were mainly formed in the source concrete of RA-R-2 before crushing it at an expansion of 3.0 ‰. Despite this, all ASR products in concrete C2 display an increased back-scattering contrast and contain Cs

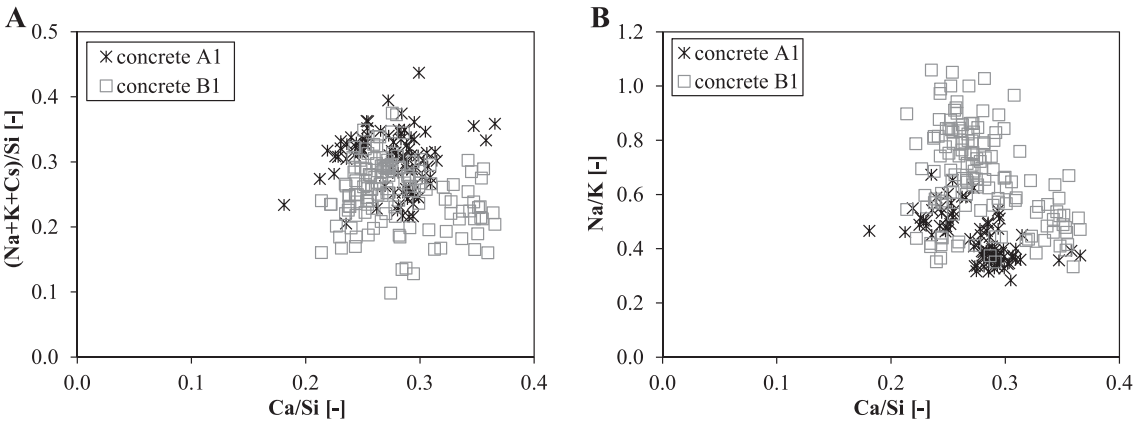

Fig. 11. (Na + K + Cs)/Si-ratio as a function of Ca/Si-ratio (A) and Na/K-ratio as a function of Ca/Si-ratio of amorphous and cryptocrystalline ASR products formed in aggregates of concrete A1 and B1 after 20 weeks.

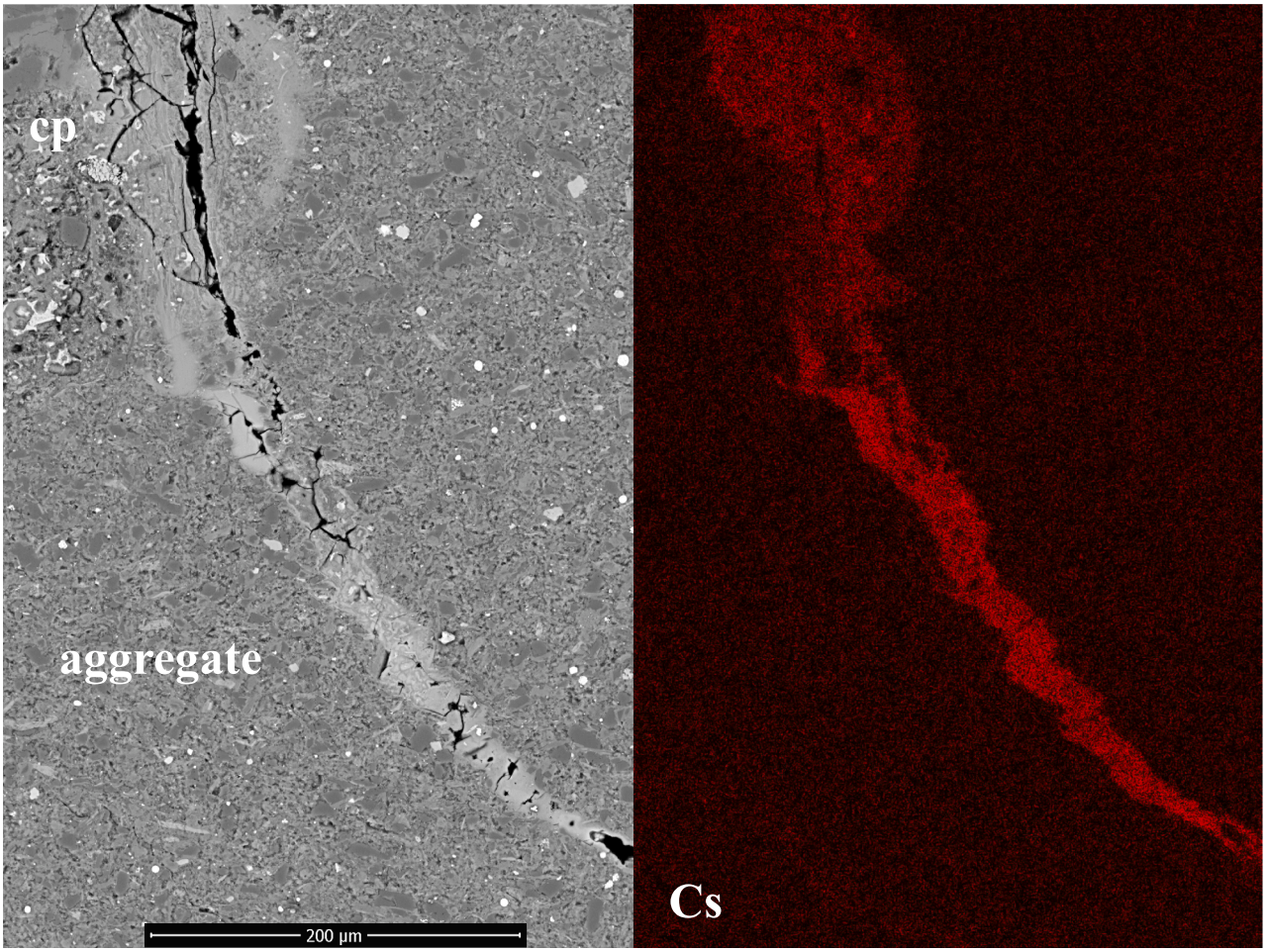

Fig. 12. Crack filled with amorphous ASR products running from the aggregate into the cement paste (cp) within a particle of aggregate RA-R-2 (left). The element map of Cs shows the identical location (right). Concrete C2 at 6 weeks. Cs added to the mixing water.

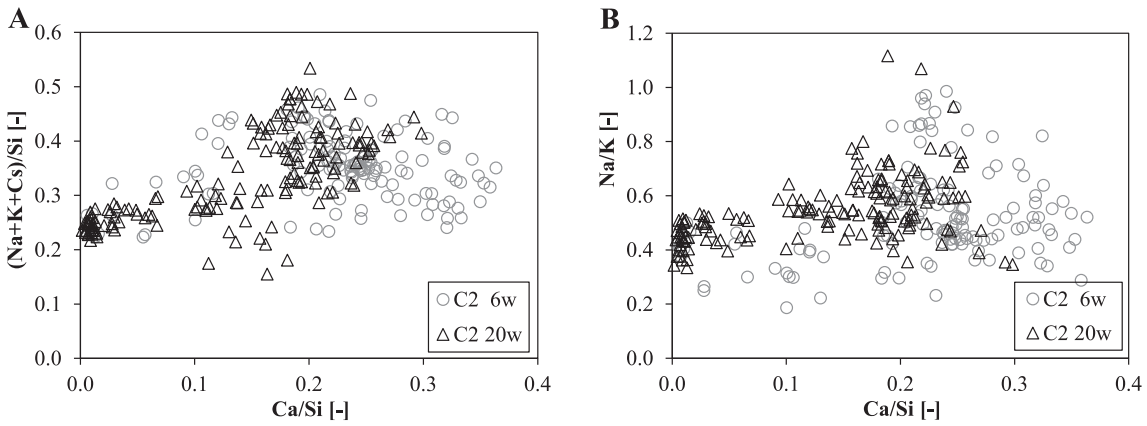

Fig. 13. (Na + K + Cs)/Si-ratio as a function of Ca/Si-ratio (A) and Na/K-ratio as a function of Ca/Si-ratio of ASR products formed in aggregates of concrete C2 after 6 and 20 weeks.

as confirmed by EDS (Table 7, Fig. 12). The Cs content is similar to the one of the ASR products formed in concrete mixture B1 corresponding the identical Cs content (34 mol/m^3). After 20 weeks, the ASR products in aggregates of concrete mixture C2 exhibit a lower average Ca/Si-ratio than after 6 weeks (Fig. 13). Additionally, there are two groups of points differing by their Ca/Si-ratio, one of them with very low values (i.e., <0.1).

4. Discussion

4.1. Pore solution

Mortar MC contains a Na_2O_{eq} of 4.92 kg/m^3 from the new cement paste and 0.60 kg/m^3 from the cement paste present in RA-NR, if only Na and K are considered. The Cs present in RA-R1 adds another 0.23 kg/m^3 of Na_2O_{eq}. If these amounts are transferred to molar concentrations this equals 178.0 mol/m^3 for Na and K and 7.5 mol for Cs resulting in a molar ratio of 23.7. The molar ratio between the sum of Na and K to Cs measured in the pore solution as presented in Table 6 ranges from 13.5 to 22.5 with an average of 18.6. Consequently, the ratio present in the components of the mortars and the ones in the pore solution are in a similar order of magnitude. The presence of Cs in the pore solution already after one day clearly indicates that alkalis from the RA are readily available in the pore solution. It can be assumed that there is an equilibration by diffusion between the alkalis present in the RA and the one in the new cement paste.

4.2. Concrete expansion

4.2.1. Scenario A

In concrete A1, aggregate RA-NR increases the alkali level resulting in a higher expansion of concrete A1 than concrete A3 where no alkali addition due to RA occurs. The Cs present in the ASR products formed in concrete A1 proofs that an equilibration between the pore solution of the new cement paste and one of the RA takes place as already indicated in the pore solution data. Despite the higher Na_2O_{eq} of concrete A2 compared to A3 (Table 4), their expansion is the same. This may be attributed to the repeatability of the method (Section 2.2).

4.2.2. Scenario B

The Na_2O_{eq} values of concrete mixtures B1 and B2 are very close, resulting in very similar induced expansion. The only difference between the two concrete mixtures is that the expansion at four weeks was higher for concrete mixture B1. As the sand fraction of aggregate RA-R-1 is only present in concrete mixture B1, its faster expansion may be attributed to fast reaction within the reactive sand fraction. In any case, the expansion caused by the recycled aggregate RA-R-1, originally containing a low alkali level, shows that alkalis present in the new cement paste may trigger ASR.

4.2.3. Scenario C

The lower expansion of concrete mixture C1 when compared to C2 can be explained by the equilibration of the alkalis between the new cement paste and the cement paste present in the RA particle. ASR in concrete mixture C1 mainly relays on the alkalis initially present in the recycled aggregate RA-R-2. Otherwise, the alkali content of the new cement paste in concrete mixture C2 is slightly higher than the one in aggregate RA-R-2, boosting a further reaction.

4.3. Microstructure

The crystalline ASR product formed in concrete mixture A1 is likely shlykovite that is typically formed in aggregates when the concrete is exposed to 60 °C [26,28]. Both the crystalline and the amorphous ASR products contain similar amount of Cs indicating the same binding capacity. The lower K and higher Cs content of the ASR products in concrete mixture B1 when compared to concrete mixture A1 clearly indicates that Cs can substitute K in ASR products. K and Cs have a similar ion radius [29] enabling this substitution.

The presence of Cs in the ASR products of concrete mixture C2 after 6 weeks shows that the pore solution of the new cement paste and the one of the RA equilibrates relatively fast. Moreover, it highlights that ASR products already present in the RA at the time of concrete production are able to sorb Cs. The lower K content of the ASR products of concrete mixture C2 when compared to C1 shows that the Cs substitutes K as already shown in the comparison between concrete mixtures A1 and A2 with B1.

Typically, the Ca/Si-ratio of ASR products increases as a function of time [30]. In the case of concrete mixture C2 the opposite is observed. The ASR products present in aggregate RA-R-2 have a higher Ca/Si-ratio after 6 weeks than after 20 weeks. This can be explained by the fact that the majority of the ASR products present at 6 weeks were formed in the source concrete of aggregate RA-R-2 crushed at the age of 23 weeks. Consequently, these ASR products exhibit a relatively high Ca/Si-ratio. The ASR products formed between 6 and 20 weeks have a lower Ca/Si-ratio leading to a lower average value (Table 7) and two groups in the ratio plots (Fig. 13).

4.4. General considerations

The Na_2O_{eq} of RC is mainly governed by the alkalis present in the new cement paste. However, the use of a recycled aggregate with a high

alkali content can increase expansion (scenario A). The potential for an increase of expansion seems to be limited, because the volume of cement paste present in RA is lower than the one of the new cement paste (Table 4). The potential for expansion is higher when reactive RA with a low alkali level is used for a recycling concrete with a high alkali level, thus triggering ASR (scenario B). The expansion potential is likely increasing with the amount of reactive RA used. The highest risk seems to be present when the source of RA is a concrete already damaged by ASR (scenario C). Even a low alkali content in the new cement paste seems not to be able to suppress expansion. Therefore, supplementary cementitious materials such as fly ash, silica fume or metakaolin should be used to avoid expansion and damage. However, SCMs seem to be less effective to prevent ASR in RC when compared to concrete with natural aggregates [9,10,12]. The duration between the crushing of the demolished concrete and its reuse as RA in RC is in the range of two months in Switzerland. Such a time span makes only ASR tests with a duration of a few weeks feasible to assess the reactivity of RA. ASR tests such as the accelerated mortar bar tests [31–33] can be used to identify reactive RA. However, the way RA are prepared to conduct accelerated ASR tests can impact on the measured expansion and an adaptation of the test protocol has to be considered [12,34]. In addition to the reactivity of the RA, their soluble alkali content may be also determined. There are several techniques that can be used for such a determination [35,36]. Results from these types of tests are typically available within days.

Additional process steps in the production of RA to reduce the cement paste content as summarized in [37,38] would lead to a lower alkali content of the RA. However, as the new cement is the main source of alkalis in the RC and as the reuse of all concrete components is in the interest of circular material flow [39–41] this seems to be an unnecessary measure.

5. Conclusions

RC mixtures were produced exploring three scenarios of different alkali levels of the new cement paste and the cement paste of the RA as shown in Fig. 1. $CsNO_3$ added to specific concrete mixtures was used as a tracer to follow alkali transport. Expansion was determined with the CPT and the composition of the ASR products in selected RC was analyzed with SEM and EDS. Additionally, pore solution extraction of two mortars was performed. The results allow to draw the following conclusions:

- The alkalis present in the RA are instantly available in the pore solution as per its composition observed after 1 day.
- An equilibration between the pore solution of the new cement paste and the cement paste of the RA takes place by diffusion.
- The alkali equilibration can impact ASR in RC containing RA and natural aggregates in several ways:
  - o Scenario A: RA containing non-reactive aggregates and a high alkali level can trigger ASR in an RC with a moderate alkali level containing reactive natural aggregates.
  - o Scenario B: RA containing reactive natural aggregates with a low alkali level can cause ASR in an RC with a high alkali level of the new cement paste.
  - o Scenario C: RA with reactive natural aggregates and high alkali level and signs of ASR, lead to ASR-induced expansion even in RC with a low-alkali level of the new cement paste. ASR is further boosted when the RC has a high alkali level.
- Consequently, both the potential reactivity of the RA and its alkali level should be known if ASR is suspected to be an issue in a new concrete.

Due to the relatively short time span of RA in a concrete plant prior to their use, only accelerated ASR tests with a duration of a few weeks should be considered to assess the reactivity of RA. Further research is still required to assess the reliability of such tests to evaluate ASR derived from RA.

CRediT authorship contribution statement

Andreas Leemann: Conceptualization, Formal analysis, Funding acquisition, Investigation, Methodology, Project administration, Resources, Validation, Visualization, Writing – original draft. **Leandro Sanchez:** Visualization, Writing – original draft, Writing – review & editing.

Declaration of competing interest

The authors declare the following financial interests/personal relationships which may be considered as potential competing interests: Andreas Leemann reports financial support was provided by cemsuisse.

Data availability

Data will be made available on request.

Acknowledgment

The authors would like to acknowledge cemsuisse for financing the project and Cassandra Trottier for the production of RA-R-2. Additionally, the authors would like to thank the two anonymous peer reviewers for their work.

References

[1] C. Zhang, M. Hu, X. Yang, B. Miranda-Xicotencatl, B. Sprecher, F. Di Maio, X. Zhong, A. Tukker, Upgrading construction and demolition waste management from downcycling to recycling in the Netherlands, J. Clean. Prod. 266 (2020) 121718.
[2] C.P. Ginga, J.M.C. Ongpeng, M.K.M. Daly, Circular economy on construction and demolition waste: a literature review on material recovery and production, Materials 13 (2020) 2970.
[3] A. Bonoli, S. Zanni, F. Serrano-Bernardo, Sustainability in building and construction within the framework of circular cities and European new green deal. The contribution of concrete recycling, Sustainability 13 (2021) 2139.
[4] V.W.Y. Tam, M. Soomro, A.C.J. Evangelista, A review of recycled aggregate in concrete applications (2000–2017), Constr. Build. Mater. 172 (2018) 272–292.
[5] M. Etxeberria, E. Vázquez, A. Marí, M. Barra, Influence of amount of recycled coarse aggregates and production process on properties of recycled aggregate concrete, Cem. Concr. Res. 37 (2007) 735–742.
[6] C. Hoffmann, S. Schubert, A. Leemann, M. Motavalli, Recycled concrete and mixed rubble as aggregates: influence of variations in composition on the concrete properties and their use as structural material, Constr. Build. Mater. 35 (2012) 701–709.
[7] A. Leemann, R. Loser, Carbonation resistance of recycled aggregate concrete, Constr. Build. Mater. 204 (2019) 335–341.
[8] X. Li, D.L. Gress, Mitigating alkali–silica reaction in concrete containing recycled concrete aggregate, Transp. Res. Rec. 1979 (2006) 30–35.
[9] M.H. Shehata, C. Christidis, W. Mikhaiel, C. Rogers, M. Lachemi, Reactivity of reclaimed concrete aggregate produced from concrete affected by alkali–silica reaction, Cem. Concr. Res. 40 (2010) 575–582.
[10] M.P. Adams, Alkali-silica Reaction in Concrete Containing Recycled Concrete Aggregates, Oregon State University, 2012.
[11] M. Piersanti, M. Shehata, S. Senior, Expansion of concrete containing recycled concrete aggregate suffering different levels of alkali-silica reaction, in: 4th International Engineering Mechanics and Materials Conference Regina, Canada, 2015, pp. 1–8.
[12] R. Johnson, M.H. Shehata, The efficacy of accelerated test methods to evaluate alkali silica reactivity of recycled concrete aggregates, Constr. Build. Mater. 112 (2016) 518–528.
[13] Z. Peng, C. Shi, Z. Shi, B. Lu, S. Wan, Z. Zhang, J. Chang, T. Zhang, Alkali-aggregate reaction in recycled aggregate concrete, J. Clean. Prod. 255 (2020) 120238.
[14] M. Barreto Santos, J. De Brito, A. Santos Silva, A review on alkali-silica reaction evolution in recycled aggregate concrete, Materials 13 (2020) 2625.
[15] M. Barreto Santos, J. de Brito, A. Santos Silva, A. Hawreen, Evaluation of alkali-silica reaction in recycled aggregates: the applicability of the mortar bar test, Constr. Build. Mater. 299 (2021), 124250.
[16] C. Trottier, A. Zahedi, R. Ziapour, L. Sanchez, F. Locati, Microscopic assessment of recycled concrete aggregate (RCA) mixtures affected by alkali-silica reaction (ASR), Constr. Build. Mater. 269 (2021), 121250.
[17] C. Trottier, R. Ziapour, A. Zahedi, L. Sanchez, F. Locati, Microscopic characterization of alkali-silica reaction (ASR) affected recycled concrete mixtures

induced by reactive coarse and fine aggregates, Cem. Concr. Res. 144 (2021) 106426.
[18] S. 262-1, Betonbau - Ergänzende Festlegungen, Schweizerischer Ingenieur- und Architektenverein, 2019.
[19] P.J. Nixon, I. Sims, RILEM recommended test method: AAR-4.1—detection of potential alkali-reactivity—60 °C test method for aggregate combinations using concrete prisms, in: P.J. Nixon, I. Sims (Eds.), RILEM Recommendations for the Prevention of Damage by Alkali-aggregate Reactions in New Concrete Structures: State-of-the-art Report of the RILEM Technical Committee 219-ACS, Springer Netherlands, Dordrecht, 2016, pp. 99–116.
[20] A. Zahedi, C. Trottier, L.F.M. Sanchez, M. Noël, Condition assessment of alkali-silica reaction affected concrete under various confinement conditions incorporating fine and coarse reactive aggregates, Cem. Concr. Res. 153 (2022), 106694.
[21] ASTMC1293, Standard Test Method for Determination of Length Change of Concrete Due to Alkali-silica Reaction, 2020.
[22] CSA-A23.2-14A, Potential Expansivity of Aggregates; Procedure for Length Change Due to Alkali-aggregate Reaction in Concrete Prisms, 2014.
[23] E. 12390-3, Testing Hardened Concrete - Part 3: Compressive Strength of Test Specimens, 2019.
[24] G. Frenzer, J.G. Hammerschlag, T. Henoch, A. Leemann, P. Lunk, C. Pilloud, G. Rytz, M. Romer, G. Spicher, C. Thalmann, H. Widmer, Alkali-Aggregat-Reaktion (AAR) in der Schweiz, cemsuisse, Verband der Schweizerischen Cementindustrie, Bern, Switzerland, 2005.
[25] A. Corneille, Results of a round robin test program for the validation of the test methods in the French recommendations for the prevention of AAR damage to concrete, ACI Spec. Publ. 145 (1994) 725–740.
[26] A. Leemann, Z. Shi, J. Lindgård, Characterization of amorphous and crystalline ASR products formed in concrete aggregates, Cem. Concr. Res. 137 (2020) 106190.
[27] A. Leemann, B. Münch, The addition of caesium to concrete with alkali-silica reaction: implications on product identification and recognition of the reaction sequence, Cem. Concr. Res. 120 (2019) 27–35.
[28] I. Fernandes, A. Leemann, B. Fournier, E. Menendez, J. Lindgård, I. Borchers, J. Custódio, PARTNER project post-documentation study. Condition assessment of field exposure site cubes. Results of microstructural analyses, Cem. Concr. Res. 162 (2022) 107006.
[29] B.E. Conway, Ionic Hydration in Chemistry and Biophysics, 1981.
[30] A. Leemann, Impact of different added alkalis on concrete expansion due to ASR, in: A. Lopes Batista, A. Santos Silva, I. Fernandes, L. Oliveira Santos, J. Custódio, C. Serra (Eds.), 16th ICAAR Lisbon, 2022, pp. 129–136.
[31] ASTMC1260, Standard Test Method for Potential Alkali Reactivity of Aggregates (Mortar-bar Method), 2022.
[32] ASTMC1567, Standard Test Method for Determining the Potential Alkali-silica Reactivity of Combinations of Cementitious Materials and Aggregate (Accelerated Mortar-bar Method), 2021.
[33] CSA23.2-25A, Test Method for Detection of Alkali-silica Reactive Aggregate by Accelerated Expansion of Mortar Bar, 2014.
[34] M. Adams, A. Jones, S. Beauchemin, R. Johnson, B. Fournier, M. Shehata, J. Tanner, J. Ideker, Applicability of the accelerated mortar bar test for alkali-silica reactivity of recycled concrete aggregates, Adv. Civ. Eng. Mater. 2 (2013) 78–96.
[35] G. Plusquellec, M.R. Geiker, J. Lindgård, J. Duchesne, B. Fournier, K. De Weerdt, Determination of the pH and the free alkali metal content in the pore solution of concrete: review and experimental comparison, Cem. Concr. Res. 96 (2017) 13–26.
[36] G. Plusquellec, M.R. Geiker, J. Duchesne, J. Lindgård, K. De Weerdt, Review of methods to determine the pH and the free alkali content of the pore solution in concrete, in: 15th ICAAR Sao Paulo, Brasil, 2016.
[37] B. Wang, L. Yan, Q. Fu, B. Kasal, A comprehensive review on recycled aggregate and recycled aggregate concrete, resources, Conserv. Recycl. 171 (2021), 105565.
[38] C. Shi, Y. Li, J. Zhang, W. Li, L. Chong, Z. Xie, Performance enhancement of recycled concrete aggregate – a review, J. Clean. Prod. 112 (2016) 466–472.
[39] A. Akhtar, A.K. Sarmah, Construction and demolition waste generation and properties of recycled aggregate concrete: a global perspective, J. Clean. Prod. 186 (2018) 262–281.
[40] Y. Yu, D.M. Yazan, S. Bhochhibhoya, L. Volker, Towards circular economy through industrial symbiosis in the Dutch construction industry: a case of recycled concrete aggregates, J. Clean. Prod. 293 (2021) 126083.
[41] A.T.M. Marsh, A.P.M. Velenturf, S.A. Bernal, Circular economy strategies for concrete: implementation and integration, J. Clean. Prod. 362 (2022) 132486.